HHS Public Access

Author manuscript

Br J Haematol. Author manuscript; available in PMC 2020 February 01.

Published in final edited form as:

Br J Haematol. 2019 February ; 184(4): 578–593. doi:10.1111/bjh.15669.

Mesenchymal stem cells gene signature in high-risk myeloma bone marrow linked to suppression of distinct IGFBP2-expressing small adipocytes

Syed J. Mehdi[1], **Sarah K. Johnson**[1], **Joshua Epstein**[1], **Maurizio Zangari**[1], **Pingping Qu**[2], **Antje Hoering**[2], **Frits van Rhee**[1], **Carolina Schinke**[1], **Sharmilan Thanendrarajan**[1], **Bart Barlogie**[1], **Faith E. Davies**[1], **Gareth J. Morgan**[1], and **Shmuel Yaccoby**[1]

[1]Myeloma Institute, University of Arkansas for Medical Sciences, Little Rock, AR;

[2]Cancer Research and Biostatistics, Seattle, WA

Summary

Recent studies suggest that multiple myeloma (MM) induces proliferation and expansion of bone marrow (BM) mesenchymal stem cells (MSCs), but others showed that MM cells induce MSC senescence. To clarify the interaction between MM and MSCs, we exploited our established MSC gene signature to identify gene expression changes in myeloma MSCs and associated functional differences. Single MSCs from patients with MM had changes in expression of genes associated with cellular proliferation and senescence and a higher proportion of senescent cells and lower proliferative potential than those from age-matched healthy donors. Single MSCs from both sources heterogeneously express MSC genes associated with adipogenesis and osteoblastogenesis. We identified the gene encoding insulin-like growth factor-binding protein 2 (IGFBP2), an MSC gene commonly altered in high risk MM, as under-expressed. Morphologically, IGFBP2+ cells are underrepresented in MM BM compared to smouldering MM. Strong IGFBP2 and adiponectin co-expression was detected in a subset of small adipocytes. Co-culturing normal MSCs with myeloma cells suppressed MSC differentiation to adipocytes and osteoblasts, and reduced expression of IGFBP2 and adiponectin. Recombinant IGFBP2 blocked IGF1-mediated myeloma cell growth. Our data demonstrate that myeloma MSCs are less proliferative and that IGFBP2+ small adipocytes are a distinct mesenchymal cell population suppressed by myeloma.

Keywords

Myeloma; microenvironment; bone marrow; adipocytes; IGFBP2

Correspondence to: Shmuel Yaccoby, University of Arkansas for Medical Sciences, Myeloma Institute, 4301 W. Markham, Slot 776, Little Rock, AR, 72205, Phone: 501-686-8745; yaccobyshmuel@uams.edu.

Authorship contributions

S.J.M. performed the studies and was one of the writers of the paper. S.K.J. performed single-cell sorting, interpreted the data and was involved in writing the paper. M.Z., F.v.R., C.S., S.T., B.B., F.E.D. and G.J.M. provided patient materials and analysed and interpreted the data. B.B., G.J.M., and J.E. designed the research and were involved in writing the paper. P.Q. and A.H. performed biostatistics and statistical analysis. S.Y. designed and directed the research, conceptualized the work, analysed and interpreted the data, and was one of the writers of the paper.

Conflict-of-interest disclosure

The authors declare no competing financial interests.

Introduction

Bone marrow (BM) mesenchymal stem cells (MSCs) are a rare population of stem cells that give rise to lineages such as osteogenic cells, adipocytes and pericytes. MSCs and their lineages comprise heterogeneous cell populations based on their localization and molecular properties (Morrison & Scadden, 2014). The main function of these cells in BM is formation of endosteal and perivascular niches (Crane *et al*, 2017). Both of these niches are disrupted in multiple myeloma (MM), as evidenced by the presence of neoangiogenesis, osteolytic lesions, impaired haematopoiesis and immunosuppression (Yaccoby, 2010a;Vacca *et al*, 2014;Paiva *et al*, 2011;Bruns *et al*, 2012), and the changes allow a subset of MM cells to escape dormancy and proliferate (Lawson *et al*, 2015).

Most studies on MSCs in MM have used cultures of expanded MSCs or MSC lines in *in vitro* and *in vivo* models (Xu *et al*, 2018). The profiles of gene expression (Corre *et al*, 2007;Garcia-Gomez *et al*, 2014), proteins (Slany *et al*, 2014) and microRNA (Berenstein *et al*, 2015;Reagan *et al*, 2014) of cultured MSCs generated from MM patients differ from those of healthy donors. The effects of MM on MSCs and their lineages *in vivo* are extensive and only partially understood. Recent studies suggest that MM induces proliferation and expansion of MSCs (Noll *et al*, 2014;Frassanito *et al*, 2014), but other studies showed that MM cells elicit a premature senescence phenotype in MSCs (Andre *et al*, 2013). Osteoblasts and osteocytes are suppressed, particularly in areas of MM involvement (Bataille *et al*, 1991;Giuliani *et al*, 2012) and factors highly produced by these cells [e.g., CCN1 (Johnson *et al*, 2014), decorin (Li *et al*, 2008)] restrain MM growth.

BM MSCs can differentiate into adipocytes, which increase with age and are considered negative regulators of haematopoiesis (Naveiras *et al*, 2009). The effects of MM on BM adipocytes remain to be elucidated (Morris & Edwards, 2018). Although adipocytes are evident in interstitial BM and support MM growth *in vitro* (Trotter *et al*, 2016;Fairfield *et al*, 2018), adiponectin, an adipogenic factor, has been shown to induce anti-MM activity and is suppressed in MM (Fowler *et al*, 2011). Recent studies identified “regulated” adipocytes that are smaller in size than constitutively present large adipocytes (Scheller *et al*, 2015), and that function as an endocrine tissue (Cawthorn *et al*, 2014), suggesting that BM adipocytes are heterogeneous.

We recently established a signature of MSC gene expression in whole bone biopsy samples and showed that it changed in association with patients’ outcomes (Schinke *et al*, 2018). To elucidate whether these changes reflect an altered proportion of MSCs, we studied the properties of unexpanded single MSCs and exploited the MSC signature to identify a novel subset of small adipocytes whose proportion was altered with disease stage and molecularly defined risk status.

Materials and Methods

Cell and tissue samples

BM aspirates and biopsy samples were obtained from random BM (RBM) of the iliac crest or from computed tomography-guided fine-needle biopsies of magnetic resonance imaging-

defined focal lesions (FLs) of patients enrolled in our Total Therapy clinical trials (registration numbers NCT00083551, NCT00081939, NCT00572169, NCT00734877, NCT00869232) before initiation of treatment (details of these clinical trials have been reported) (Nair *et al*, 2010;van Rhee *et al*, 2014). Similarly, control samples for gene expression profiling (GEP) were obtained from BM of healthy donors (Schinke *et al*, 2018).

For MSC generation, samples were obtained from femur heads of age-matched individuals who underwent orthopaedic surgery at the University of Arkansas for Medical Sciences. All patients and donors signed written informed consent for the reported investigations and relevant clinical trial participation. All protocols were approved by the institutional review board, and clinical results have been reported annually. CD138 (SDC1)-expressing plasma cells were isolated as previously described (Zhan *et al*, 2006). MSCs were characterized as we previously described (Yaccoby *et al*, 2006;Pennisi *et al*, 2009;Li *et al*, 2011;Li *et al*, 2012).

Gene expression profiling (GEP)

GEP was performed with the Human Genome U133 Plus 2.0 Array (Affymetrix, Santa Clara, CA, USA), as previously described (Zhan *et al*, 2006; Shaughnessy, Jr. *et al*, 2007). Whole biopsies were snap-frozen in liquid nitrogen. Frozen bones were ground thoroughly in liquid nitrogen with a mortar and pestle. The tissue powder and liquid nitrogen were decanted into a cooled tube, and the liquid nitrogen was allowed to evaporate. RNA was isolated as previously described (Zhan *et al*, 2006). GEP data from MM cell samples of patients enrolled in our Total Therapy 3 (TT3) clinical trial were deposited at Gene Expression Omnibus (GEO: GSE2658). GEP-based scores used to define low-risk (LR) and high-risk (HR) MM and molecular subgroups in MM cells were previously described (Zhan *et al*, 2006; Shaughnessy, Jr. *et al*, 2007). GEP data were available for baseline BM biopsy samples from healthy donors ($n = 68$); patients with monoclonal gammopathy of undetermined significance (MGUS: $n = 38$), smouldering MM (SMM; $n = 52$), and presenting cases of LR ($n = 467$) and HR ($n = 64$) MM; and from focal lesion (FL) samples ($n = 178$). Also, paired samples (i.e., from the same patient) of RBM and FL biopsy ($n = 77$) were available.

Identification of mesenchymal stem cell (MSC) genes

Identification of MSC genes was performed as previously described (Schinke *et al*, 2018). Briefly, to identify genes that are highly expressed by MSCs in comparison to haematopoietic or MM cells, we analysed GEP data from samples of cultured MSCs ($n = 30$) (Pennisi *et al*, 2009;Li *et al*, 2012), CD138-selected MM cells from patients with MM ($n = 1227$) (Zhan *et al*, 2006; Shaughnessy, Jr. *et al*, 2007), and buffy-coats from BM aspirate samples from MM patients (enriched with haematopoietic and MM cells but not mesenchymal cells; $n = 26$). MSC genes were defined by expression signal ($\log_2$) of > 10 in cultured MSCs and < 9 in MM cells and haematopoietic cells. This approach is different than that used by Corre *et al* (2007) who identified genes differentially expressed between cultured MSCs from healthy donors and from MM patients, regardless of absolute expression in MSCs or whether they are also expressed by BM cells and MM cells.

Single-cell sorting

To isolate unexpanded MSCs, patient biopsies (n=3) and bone pieces from healthy subjects (n=3) were cut, minced and incubated (37°C, 1 h with agitation) with collagenase I and II (0.5 mg/ml each; Worthington Biochemical, Lakewood, NJ, USA) and 0.5 mM $CaCl_2$ and then cultured for 2–4 days. Cells were trypsinized to facilitate collection of MSCs without macrophages, re-plated and cultured overnight, resulting in a highly purified population of unexpanded MSCs.

Unexpanded MSCs were trypsinized and collected for single-cell sorting (FACSAria Fusion, BD Biosciences, San Jose, CA, USA). Cells were sorted into a 96-well plate, cultured overnight, stained with Carboxyfluorescein succinimidyl ester (CFSE; 0.25 μM; Sigma, St Louis, MO, USA), and visualized under a microscope to confirm the number and morphology of MSCs sorted into each well. The single MSCs were used for real time quantitative reverse transcription polymerase chain reaction (qRT-PCR) analysis.

Single-cell qRT-PCR

A total of 34 genes were selected for qRT-PCR amplification and analysis. These included MSC genes overexpressed in MM BM (*COL4A1*, *COL4A2*, *POSTN*, *FN1*, *AHR*, *CSPG4*) and MSC genes underexpressed in MM BM (*IGFBP2*, *CYBRD1*, *FOXC1*),(Schinke *et al*, 2018) as well as housekeeping genes (*GAPDH*, *ACTB*), haematopoietic cell markers (*PTPRC* [CD45], *CD34*), MSC markers (*CALD1*, *FAP*, *LEPR*, *NT5E* [CD73], *THY1* [CD90], *ALCAM*), cell cycle/proliferation markers (*CCND1*, *MKI67*, *CDKN1A*, *CDKN2A*), differentiation-associated markers (*COL1A1*, *CYR61*, *RUNX2*, *TNFRSF11B*, *PPARG*), and cytokines and chemokines (*TGFB1*, *CXCL10*, *CXCL12*, *IGF1*, *IGF2*). Gene expression was determined with the 192.24 integrated fluidic circuit, using Delta Gene assays, on a Biomark HD (Fluidigm, San Francisco, CA, USA), according to the manufacturer's protocol; data were analysed with Real-Time PCR Analysis software (Fluidigm). For each gene of each cell, delta Ct (ΔCt) was calculated by subtracting the Ct value from the mean Ct of the housekeeping genes (*GAPDH*, *ACTB*). Cells that expressed the haematopoietic cell markers (*PTPRC*, *CD34*) or low levels of the housekeeping genes were excluded from the analysis.

Single-cell MSC growth pattern and senescence assay

Wells with single cells were cultured in Minimum Essential Medium - α modification (αMEM) supplemented with 20% fetal bovine serum (FBS). Growth of single MSCs was monitored weekly with CFSE staining (0.25 μM), and images were obtained with a Zeiss AX10 Observer.A1 microscope (Carl Zeiss Microimaging Gmbh, Göttingen, Germany) equipped with an Infinity 3 camera (Lumenera, Ontario, Canada). Upon reaching ~50% confluence, cells were trypsinized and re-plated into 24-well plates to establish MSC lines from single cells. The growth patterns of single MSCs were segregated into four groups: single MSCs that remained single, single MSCs that divided only once, single MSCs that divided a few times and stopped, and single MSCs that were capable of expansion and generation of MSC lines. These lines typically grow as standard MSC cultures for a limited number of passages. Overall, 17, 18 and 24 MSC lines have been successfully generated from 3 different age-matched healthy donors, and 12, 7 and 8 MSC lines were generated

from biopsies of 3 different patients. Senescence was assessed with the cellular senescence assay kit (Cell BioLabs, San Diego, CA, USA) that detects senescence-associated β-galactosidase (SA-βGal) in cells, according to the manufacturer's protocol.

Immunohistochemistry—Immunohistochemistry (IHC) was performed in bone biopsy sections, cultured chamber slides, and lipid layer cytospin slides. After peroxidase quenching (3% hydrogen peroxide, 10 min), slides were incubated with IGFBP2 (1:500 dilution, Novus Biologicals, Littleton, CO, USA), adiponectin (2 μg/ml, LifeSpan BioSciences, Seattle, WA) and CD36 antibodies (5 μg/ml, Novus Biologicals, Littleton, CO, USA). Assays were completed with Dako LSAB2 system-horseradish peroxidase (HRP) kit (Agilent Pathology Solutions, Santa Clara, CA, USA) and counterstaining with haematoxylin. For IGFBP2 and Ig kappa or lambda double-staining, the Multi-view (mouse HRP/mouse alkaline phosphatase) IHC kit (Enzo Life sciences, Farmingdale, NY, USA) was used according the manufacturer's instructions. For sequential staining of adiponectin and IGFBP2, Doublestain IHC kit: M&R on human tissue (HRP/Green & Fast Red) was used (Abcam, Cambridge, MA, USA). To avoid false positivity, the counterstaining step with haematoxylin was omitted. An Olympus BH2 microscope (Olympus, Melville, NY, **USA**) was used to obtain images with a SPOT 2 digital camera (Diagnostic Instruments Inc., Sterling Heights, MI, USA). Adobe Photoshop version 10 (Adobe Systems, San Jose, CA, USA) was used to process the images.

Primary Adipocyte Isolation

Bone pieces collected from normal femur heads were digested with collagenase I and collagenase II (0.5 mg/ml each; Worthington Biochemical, Lakewood, NJ, USA) and 0.5 mM $CaCl_2$ at 37°C with agitation for 1 h. Following tissue digestion, the suspension was passed through a 40-μm sterile cell strainer (Fisher Scientific, Waltham, MA, USA) and centrifuged at 250*g* for 5 min. The adipocytes, which form a layer at the top of the liquid, were washed twice, placed on top of 3 μM Transwell inserts in 24-well plates (Thermo-Fisher Scientific, Waltham, MA, USA) or cytospun, and then subjected to IGFBP2 immunohistochemistry.

MSC priming

Standard cultures of MSCs were prepared as previously described (Yaccoby *et al*, 2006; Li *et al*, 2011; Li *et al*, 2012). Normal MSCs (5×10^5 cells/ml) were seeded into a 6-well plate and cultured overnight in αMEM (Gibco, Grand Island, NY, USA) containing 10% FBS and antibiotics at ~70% confluence. These MSCs were then cultured alone (unprimed MSCs) or co-cultured with MM cells (5×10^5/ml) for 3 days (primed MSCs). Primed and unprimed MSCs were trypsinized and re-plated in the 6-well plates for 40 min, and then washed 3 times to remove MM cells from co-cultures. MSCs comprised more than 95% of the remaining adherent cells after co-culture. The unprimed and primed MSCs were subjected to the following analyses: 1. qRT-PCR of several MSCs markers including *NT5E*, *THY1*/, *FAP* and *FN1*. 2. MSCs were cultured overnight in serum-free medium and the conditioned medium (CM) were collected for analysing the level of IGFBP2 secretion. 3. MSCs were re-plated in 8-well chamber slides (Thermo-Fisher Scientific, Waltham, MA, USA) or 24-well plates and subjected to adipocyte and osteoblast differentiation.

Adipocyte differentiation—Normal MSCs were plated in 8-well chamber slides (Thermo-Fisher Scientific, Waltham, MA, USA) and cultured for 3 weeks in adipogenic induction medium containing 0.5 mM isobutyl-methylxanthine (Sigma-Aldrich, St. Louis, MO, USA), 1 μM dexamethasone (Sigma-Aldrich, St. Louis, MO, USA), 10 μM insulin (Sigma-Aldrich, St. Louis, MO, USA), and 100 μM indomethacin (Sigma-Aldrich, St. Louis, MO, USA). Large adipocytes were detected with Oil Red O staining.

Osteoblast Differentiation

Primed and unprimed MSCs were re-plated in 24-well plates (Thermo-Fisher Scientific, Waltham, MA, USA) and cultured for 3 weeks in osteoblastic medium, including α-MEM medium supplemented with 10% FBS, 10 mM β-glycerophosphate (Sigma, St Louis, MO, USA), 50 μg/ml ascorbic acid (Sigma, St Louis, MO, USA) and 0.1 μM dexamethasone (Sigma, St Louis, MO, USA). For Alkaline phosphatase (ALP) activity, cells were washed with phosphate-buffered saline (PBS), fixed with 10% formaldehyde at room temperature and then stained with 5-bromo-4-chloro-3-indolyl-phosphate/nitro-blue tetrazolium solution (Sigma, St Louis, MO, USA) for 30 min at 37 °C. Calcium deposition was visualized by alizarin red S (GFS Chemicals, Columbus, OH, USA). Briefly, cells were washed with PBS, fixed with 10% formaldehyde at room temperature and then stained with 2% Alizarin Red solution (pH 4.2) for 20 min. Imaging was performed using an AMG microscope (EVOS, Millcreek, WA, USA). Next, calcium deposition was quantified using 10% (w/v) cetylpyridinium chloride in 10 mM sodium phosphate (pH 7.0), and absorbance was measured at 562 nm using spectramax 340 (Molecular Devices, San Jose, CA, USA).

Quantitative RT-PCR

Total RNA from unprimed and primed MSCs were isolated using RNeasy kit (Qiagen, Valencia, CA, USA) and cDNA was synthesized from 1 μg of total RNA using high capacity cDNA Reverse Transcriptase kit (Applied Biosystems, Foster City, CA, USA). The mRNA expression of indicated gene was quantified using SYBR Green Expression Assays on CFX Connect System (Bio-Rad, Hercules, CA, USA). The relative levels of indicated genes were calculated by using the comparative threshold cycle (CT) method after normalization to *ACTB*.

IGFBP2 secretion by MSCs.

IGFBP2 levels in serum-free CM from cultures of unprimed and primed MSCs were profiled using Quantibody Human IGF Signaling Array 1 system (RayBiotech, Norcross, GA, USA) according to the manufacturer's specifications.

Effects of recombinant IGF1 and IGFBP2 on MM cell growth

The BM-dependent MM cell lines, M, D and I were established in our laboratory as previously described (Li *et al*, 2007). To study the effects of IGFBP2 on MM cell growth, the three luciferase-expressing BM-dependent MM cell lines were cultured in serum-free αMEM for 48 h in the presence of IGF1 (40 ng/ml) and/or IGFBP2 (5 μg/ml) (R&D Systems, Minneapolis, MN, USA). After 48 h, D-Luciferin K+ Salt Bioluminescent Substrate (PerkinElmer, American Fork, UT, USA) was added to each well (1.5 mg/ml), and

the bioluminescence was measured at 175 nm with a Synergy H1 hybrid reader (BioTek, Winooski, VT, USA) as described (Li *et al*, 2007).

Statistical analyses

Significance was determined with the unpaired Student's *t* test. For each of the 469 MSC-associated probe sets identified by GEP, multiple comparison adjustments were used to calculate the q value. Values of experimental data are expressed as mean ± standard error of the mean (SEM).

For single-cell qRT-PCR analyses, adjusted ΔCt for each gene in single MSCs of healthy donors and MM sample was calculated by subtracting the ΔCt of each gene from the mean of ΔCt of total cells and data were presented as adjusted mean ΔCt ± SEM. *P* values were calculated from unpaired *t*-tests for the two samples groups (donors and MM patients) with unequal variances for each gene.

Results

Impaired adipogenesis and enhanced angiogenesis are linked to expression of MSC genes commonly altered in FLs and in BM of patients with HR MM

We examined our MSC gene expression signature (Schinke *et al*, 2018) in MM to identify critical changes in mesenchymal cell populations. The signature includes 469 MSC-associated probe sets mapped to 345 MSC genes that encode extracellular matrix (ECM) proteins, cell-surface proteins, secreted proteins, and transcription factors (Table SI). To further identify MSC genes whose expression is significantly impacted by MM, we compared MSC gene expression levels (1) in random interstitial BM biopsies of patients with molecularly-defined LR and HR MM (Shaughnessy, Jr. *et al*, 2007) and (2) in paired biopsy samples from RBM and FLs (i.e., samples from two sites collected from the same patient); 41 of the MSC genes were differentially expressed in both comparisons (Fig 1A). The genes most overexpressed were related to angiogenesis and ECM, including several collagen genes (e.g., *COL4A1*, *COL4A2*), *POSTN* and *HSPG2*. Interestingly, several under-expressed genes were associated with adipocytes, including insulin-like growth factor-binding protein 2 (*IGFBP2*) and aldo/keto reductases (e.g., *AKR1C1*, *AKR1C2*, *AKR1C3*).

To determine whether MM risk status (Shaughnessy, Jr. *et al*, 2007), disease stage or growth in FLs was associated with MSC gene expression patterns, we analysed expression of genes known to be associated with adiposity and angiogenesis, including the adipocyte-associated *IGFBP2*, which was underexpressed (Fig 1B), and angiogenesis-associated *COL4A1*, which was overexpressed (Fig 1C). We compared expression of the two genes in RBM biopsies from healthy donors and from patients with MGUS/SMM, LR MM and HR MM, and in FL biopsies. Expression of *IGFBP2* was highest in samples from healthy donors and gradually decreased to its lowest level in samples from patients with HR MM. In contrast, expression of *COL4A1* was lowest in samples from healthy donors, slightly elevated in those from MGUS/SMM, higher in those from LR and HR MM RBM, and highest in those from FLs (regardless of molecularly-defined risk). Overall, expression patterns of MSC genes in samples from patients with MGUS/SMM and LR MM were closer to those in samples from

healthy donors, while expression patterns of MSC genes in samples from patients with HR MM were closer to those in samples from FLs. These findings illustrate the significant changes in expression patterns of MSCs in interstitial BM that occur during disease progression. These data also demonstrate that FLs are niches of HR MM and indicate that MSCs and their lineages may change in similar ways in FLs from all molecularly-defined risk groups and in RBM of patients with HR MM.

Unexpanded single MSCs are heterogeneous

We hypothesized that altered expression of MSC genes in MM whole-bone samples (Schinke *et al*, 2018) reflects changes in the proportion of MSCs with this expression signature. To address this hypothesis, we sorted individual unexpanded MSCs from healthy donors and MM patients and used qRT-PCR to measure expression of selected MSC genes (Schinke *et al*, 2018) and genes associated with osteoblastogenesis and adipogenesis. We also analysed expression of *MKI67*, *CCND1*, *CDKN1A* and *CDKN2A* (p16) as markers of cellular proliferation and senescence, and we used expression of *PTPRC* and *CD34* to exclude cells of haematopoietic and endothelial origins.

We compared expression of single MSCs isolated from unexpanded bone biopsies from three healthy donors (total of 175 single MSCs) and from three patients with MM (total of 162 single MSCs) (Fig 2A). Overall, typical MSC genes, such as *COL1A1* and *FN1*, were expressed by more than 97% of normal MSCs, whereas markers associated with osteoblastic lineage (e.g., *POSTN*, *TNFRSF11B*) or adipocytic lineage (e.g., *PPARG*, *LEPR*) were expressed by fewer than 60% of normal MSCs. Factors associated with MSC differentiation to osteoblasts (e.g., *RUNX2*, *FOXC1*) and adipocytes (*PPARG*) and cell proliferation (*MKI67*) were expressed by at least 10% less MM MSCs than healthy donor MSCs, but the difference was not statistically significant.

Relative mean expression of *NT5E*, *CYR61*, *PPARG*, *TGFB1* and *MKI67* was significantly lower in single MM MSCs than from healthy donors (1.6±0.16 ΔCt values), but relative mean expression of the senescence marker (*CDKN2A*) was higher (2.0 ΔCt values; $P < 0.05$) (Fig 2B). These data demonstrate that single MSCs from either healthy donors or patients with MM have a high degree of molecular heterogeneity and that the differences in MSC signatures of healthy donors and MM patients (Schinke *et al*, 2018) cannot be explained solely by changes in gene expression of individual MSCs.

Single MSCs from MM BM are functionally quiescent—Reduced expression of *MKI67* and increased expression of *CDKN2A* in single MM MSCs indicates that patients' MSCs have impaired proliferative potential. To investigate this possibility, we examined the ability of single MSCs to proliferate *in vitro*. The growth pattern of single MSCs was segregated into four groups: MSCs that did not divide, MSCs that divided only once, MSCs that underwent a few cell divisions and stopped, and MSCs that were capable of continued expansion (*i.e.* MSC lines) (Fig 3A). Compared to single MSCs from healthy donors, a higher proportion of MSCs from MM patients did not divide, and fewer were capable of limited proliferation or generating an MSC line (Fig 3B). Moreover, a higher proportion of MSCs from MM patients expressed the senescence marker, SA-βGal (Fig 3C, D). Thus,

under the indicated culture conditions, MM patients' MSCs are less likely to be proliferative or differentiate, which led us to hypothesize that the MM-associated differences in MSC gene expression (Schinke *et al*, 2018) reflect modifications in mesenchymal cell lineages that encompass most of the mesenchymal compartment in bone.

Low levels of IGFBP2 reflect reduced proportions of small adipocytes that produce IGFBP2 in BM of patients with MM

IGFBP2 is secreted by adipocytes and is implicated in bone homeostasis and adiposity (Xi *et al*, 2014;DeMambro *et al*, 2015;Rahman *et al*, 2013;Boney *et al*, 1994), and its levels are lower in BM than in blood of MM patients (Bieghs *et al*, 2016a). We hypothesized that IGFBP2 could serve as a biomarker of BM adiposity. To address this hypothesis, we used immunohistochemistry to trace the cellular source of IGFBP2 in BM biopsy samples, and analysed the relationship to IGF1-induced MM cell growth.

IGFBP2+ cells were clearly evident in BM biopsies from patients with MGUS/SMM compared to patients with active MM. IGFBP2+ cells morphologically resembled MSCs and the small adipocytes that are frequently detected in clusters in areas enriched with haematopoiesis. Large, mature adipocytes were negative to weakly positive for IGFBP2. The smooth muscle cells that cover well-established arteries also were IGFBP2+ (not shown). The number of IGFBP2+ cells was higher in BM biopsies from patients with MGUS/SMM than in those from patients with MM, and the number was lower in biopsies from patients with HR MM than with LR MM (Fig 4A, B). In cases with samples from multiple areas from the same patient, IGFBP2+ cells were evident in the uninvolved area but not in areas highly infiltrated with MM cells (Fig 4C, D). These results suggest that IGFBP2 is a marker of a subpopulation of small adipocytes whose proportion in BM is reduced during disease progression.

To confirm that IGFBP2+ cells are mainly adipocytes, biopsy samples from healthy donors and MGUS/SMM patients were stained for adiponectin or were sequentially stained for adiponectin and IGFBP2. Adiponectin reactivity was more evident in small adipocytes than in large adipocytes (Fig 5A). Sequential staining revealed that small adipocytes were heterogeneous in levels of IGFBP2, adiponectin and co-expression of both markers (Fig 5B). These data indicate that adipocytes (particularly small adipocytes) produce high levels of IGFBP2 in BM.

Next, we further examined IGFBP2 expression in adipocytes. Cultured normal MSCs were differentiated into adipocytes, and both cell types were immunohistochemically stained for IGFBP2 and the adipocyte markers, adiponectin and CD36 (Mattiucci *et al*, 2018). Undifferentiated MSCs were negative for adiponectin and CD36 but had low level of IGFBP2. In contrast, differentiated adipocytes showed strong staining in all three markers (Fig 6A). GEP analysis of MSCs before and after differentiation into adipocytes confirmed marked upregulation of genes encoding all three proteins (Fig 6B). In addition, primary small adipocytes from healthy donor BM (isolated by cytospin or Transwell filters) were positive for IGFBP2 (Fig 6C). These findings further validate that adipocytes are the primary source of IGFBP2.

Priming MSCs with MM cells suppresses their differentiation to adipocytes and reduces their expression of IGFBP2

To test whether MM cells affect MSC differentiation into adipocytes and cause the reduction in IGFBP2, we primed normal MSCs with MM cells and then examined the effects on their ability to differentiate to adipocytes and to express *IGFBP2*. Expression of the MSC genes, such as *NT5E*, *THY1*, *FAP* and *FN1*, was similar between unprimed and primed MSCs (Fig S1.). However, priming MSCs by co-culturing them with MM cells for 3 days resulted in substantially suppressed differentiation into lipid-containing large adipocytes (Fig 7A) or osteoblasts (Fig S2.). Furthermore, priming MSCs by culturing them in standard culture medium or in adipogenic induction medium resulted in lower IGFBP2 and adiponectin levels in MSCs that had been cultured with MM than those that were cultured alone (Fig 7B). To determine whether cell-cell contact is necessary for IGFBP2 downregulation, normal MSCs were cocultured with MM cells with and without culture inserts that block cell-cell contact. Cell-cell contact resulted in marked suppression of *IGFBP2* in MSCs, whereas expression of *IGFBP2* was only partially inhibited without cell-cell contact (Fig 7C). Conditioned media from MSCs primed by direct contact with MM cells also had lower levels of IGFBP2 protein (Fig 7D). These data suggest that reduced production of *IGFBP2* in bones of patients with MM is mediated through suppression of adipocyte differentiation and direct contact with MM cells.

IGFBP2 blocks the stimulatory effects of IGF1 on MM cell growth

Although the IGF axis is centrally involved in MM growth and has been extensively studied (Bieghs *et al*, 2016b), the effects of IGFBP2 on MM cell growth have not been reported. Among the seven IGFBPs, only *IGFBP2* is underexpressed in biopsy samples from MM patients compared to those from healthy donors (Fig 8A). *IGF1* is overexpressed, whereas *IGF2* and the gene encoding its transcription factor enhancer, *IGF2BP2* (Bell *et al*, 2013), are underexpressed in myelomatous bones (Fig 8A). *IGF1*, but not *IGF2*, is expressed also by MM cells and reportedly is abundant in the MM microenvironment (Bieghs *et al*, 2016b). We therefore focused our functional test on IGF1 and showed that recombinant IGF1 significantly promoted short-term growth of three microenvironment-dependent MM cell lines cultured alone, without support from microenvironment cells (Fig 8B). Recombinant IGFBP2 had no direct effect on growth but markedly abrogated the growth-stimulatory effects of recombinant IGF1 of these MM cell lines (Fig 8B). These data suggest that reduced levels of IGFBP2 in the MM microenvironment result in increased bioavailability of IGF1 and IGF1-induced cell growth.

Discussion

In this work, we provide evidence that the BM of MM patients contains fewer MSCs with proliferative potential and fewer MSCs that express genes associated with their osteogenic or adipogenic differentiation potential. Using the MSC gene signature that we established (Schinke *et al*, 2018), we further identified IGFBP2-expressing cells as a subset of adipocytes that is reduced as the disease progressed from MGUS to LR and HR MM. Co-culturing MSCs with MM cells inhibited their differentiation into adipocytes and osteoblasts, and reduced IGFBP2 expression and secretion. IGFBP2 effectively blocked the

ability of IGF1 to stimulate MM cell growth. These results suggest that, in addition to inhibition of osteoblastogenesis (Yaccoby, 2010b), MM also inhibits formation of small adipocytes, a cell population that is closely associated with red marrow and haematopoiesis (Scheller *et al*, 2015). Our findings also indicate that, similar to other mesenchymal cell factors, such as decorin, CYR61, and adiponectin (Li *et al*, 2008;Fowler *et al*, 2011;Johnson *et al*, 2014), IGFBP2 functions as a MM-restraining factor that is suppressed during disease progression.

We found the expression patterns of MSC genes in FLs from all risk groups were similar to those of MSCs in BM of patients with HR MM and that expression of most MSC genes was lower in FLs and in HR MM than in LR MM. Most overexpressed MSC genes are related to ECM and angiogenesis (e.g., *COL4A1*, *POSTN*), while underexpressed MSC genes are associated with a diverse range of cellular and biological activities of BM mesenchymal cells (e.g., transcription factors *HOX10A*, *HOXB2*, *NFIX*, *FOXC1*) and with adipogenic lineage (e.g., *IGFBP2*, *AKR1C3*). Reduced *IGFBP2* expression is linked to a reduced proportion of small adipocytes – a distinct BM mesenchymal cell population that has not been implicated in MM pathogenesis. These findings highlight the role of FLs as a niche for HR MM and the possible involvement in MM progression of small adipocytes that produce high levels of factors, such as IGFBP2 and adiponectin.

To our knowledge, this is the first study to characterize MSC heterogeneity at the single-cell level in MM. The proportion of cells expressing MSC genes ranged from 99% (e.g., *FN1*) to 25% (*POSTN*) of normal MSCs. It was previously shown that individual MSCs heterogeneously express markers, such as *THY1*, *NT5E* and *LEPR* (Lv *et al*, 2014). Most of the examined genes were not expressed differentially by individual MSCs from normal subjects compared to patients with MM. Nevertheless, single MSCs derived from MM had reduced proportions and mean levels of expression of genes related to proliferation (e.g., *MKI67*) and differentiation (e.g., *RUNX2, PPARG*), and increased expression of senescence marker *CDKN2A*. These changes in gene expression are associated with reduced proliferative potential of single MSCs in long-term cultures, supporting the speculation that MM cells directly induce a premature senescence phenotype in MSCs (Andre *et al*, 2013).

The reduction in osteoblast numbers (Bataille *et al*, 1991) and increase in osteocyte apoptosis (Giuliani *et al*, 2012) in areas infiltrated with MM cells is well documented, but the involvement of other mesenchymal cell types, such as adipocytes and pericytes, is poorly defined *in vivo*. In this context, the adipogenic factor adiponectin inhibits MM cell growth and is suppressed in the BM of MM (Fowler *et al*, 2011). IGFBP2 has been shown to act either as an oncogene or tumour suppressor, depending on tumour type and cellular context (Pickard & McCance, 2015). Here, we show that IGFBP2 is highly expressed by small adipocytes, but not by mature adipocytes, within the BM. The number of IGFBP2+ cells is markedly reduced in FLs and in RBM of patients with HR MM. The reduced numbers of small adipocytes in MM might be induced through multiple mechanisms. First, as we have shown, the interaction of MM cells with MSCs leads to induction of senescence in MSCs and suppression of differentiation into adipocytes. This effect could be reversible depending the duration and intensity of MM cells-MSCs interaction (Dabbah *et al*, 2016). Second, a subpopulation of distinct BM-”regulated” small adipocytes that are metabolically active and

systemically regulated in physiological conditions (Scheller *et al*, 2015) may be suppressed by MM. Third, as shown in a 3-dimensional model of adipocyte-MM cell interaction, MM cells may use fatty acids in adjacent large adipocytes, causing the large cells to shrink and eventually be eliminated in areas highly involved with MM (Fairfield *et al*, 2018), as documented in our work.

Our results suggest that mesenchymal cells play a critical role in orchestrating the activity of IGFs in the BM niches. IGF1 is abundant in myelomatous bone and is produced by MM cells and microenvironmental cells (Bieghs *et al*, 2016b). Our data indicate that mesenchymal cells are a major producer of IGF2 and IGF-binding proteins in BM, and that levels of IGF2 and IGFBP2 are suppressed in HR MM. IGFBP2 promotes osteoblast differentiation via IGF-dependent and -independent mechanisms (Xi *et al*, 2014), and loss of IGFBP2 resulted in increased bone resorption in male mice, with similar effects in ovariectomized female mice (DeMambro *et al*, 2015;DeMambro *et al*, 2008). Additionally, IGFBP2 is important for maintaining the haematopoietic stem cell niches in BM and in supporting haematopoietic stem cell survival and cycling (Huynh *et al*, 2011;Kobayashi *et al*, 2010). Other studies showed that cleavage of IGFBPs by proteases also contributes to enhanced IGF1 bioavailability (Baxter, 2014), suggesting that reduced levels of IGFBP2 in BM of patients with MM (Bieghs *et al*, 2016a) resulted from multiple mechanisms. It is likely that the changes in multiple factors related to the IGF axis in FLs and in the microenvironment of HR MM result in increased bioavailability of IGF1 and reduced bioavailability of IGF2. These changes may promote survival and growth of MM cells directly and, through induction of MM bone disease, indirectly.

The identification of regulatory small adipocytes and constitutive large adipocytes in BM (Scheller *et al*, 2015) may partially explain contradictory reports about the role of BM adipocytes in regulating haematopoiesis and tumourigenesis. While increased adiposity in BM is regarded as inhibitory for haematopoiesis (Naveiras *et al*, 2009), other studies show that adipocytes produce critical factors that promote haematopoiesis, such as adiponectin (Cawthorn *et al*, 2014) and stem cell factor (Zhou *et al*, 2017). Acute myeloid leukaemia (AML) interrupts adipogenesis in red BM, leading to compromised myelo-erythroid maturation, which is negated by PPARG agonists, and repressed leukaemic growth (Boyd *et al*, 2017). In contrast, BM adipocytes are induced by AML (Shafat *et al*, 2017) and MM cells (Fairfield *et al*, 2018) to increase lipolysis, resulting in release of fatty acids that are used by tumour cells. Therefore, understanding the functions of small and large adipocytes is clinically relevant with regard to understanding the roles of BM microenvironment in MM progression and to designing successful immune-based therapies. Obesity induced by a high-fat diet is associated with increased numbers and sizes of BM adipocytes (Scheller *et al*, 2016;Doucette *et al*, 2015). Obese patients with MGUS are more likely to progress to MM (Landgren *et al*, 2010), and lysolipids have been shown to be the source of antigenic origins in a subset of patients (Nair *et al*, 2016). In contrast, caloric restriction causes a dramatic expansion of small adipocytes in BM and increased adiponectin levels (Cawthorn *et al*, 2014). Circulating adiponectin levels are inversely correlated with MGUS progression to MM (Fowler *et al*, 2011). Therapy also may impact BM adiposity. In a model of glucocorticoid-induced osteoporosis, chronic glucocorticoid treatment, as is often used in MM therapy, initially was associated with increased numbers of small adipocytes in BM,

followed by adipocyte hyperplasia and severe osteoporosis later on (Li *et al*, 2013). Data from patients undergoing therapy for ovarian or endometrial cancer showed that these patients display expansion of adipocytes in lumbar vertebral marrow and elevated serum levels of adiponectin, despite no change in total adiposity (Cawthorn *et al*, 2014). Thus, developing approaches to increase the number of BM regulatory small adipocytes and simultaneously prevent adipocyte hypertrophy may help control MM.

In summary, we show that expression of distinct MSC genes is altered in sites involved with focal growth of MM cells and in interstitial BM of patients with HR MM. These genes are differentially expressed by distinct subpopulations of mesenchymal cells, such as small adipocytes, and are altered at different stages of the disease.

Supplementary Material

Refer to Web version on PubMed Central for supplementary material.

Acknowledgments

We wish to thank the faculty, staff and patients of the Myeloma Institute for their support. We also thank the Science Communication Group at the University of Arkansas for Medical Sciences for editorial assistance during the preparation of this manuscript. This work was supported by a grant from the National Cancer Institute (CA55819).

References

Andre T, Meuleman N, Stamatopoulos B, De BC, Pieters K, Bron D, & Lagneaux L (2013) Evidences of early senescence in multiple myeloma bone marrow mesenchymal stromal cells. PLoS One, 8, e59756. [PubMed: 23555770]

Bataille R, Chappard D, Marcelli C, Dessauw P, Baldet P, Sany J, & Alexandre C (1991) Recruitment of new osteoblasts and osteoclasts is the earliest critical event in the pathogenesis of human multiple myeloma. J Clin Invest, 88, 62–66. [PubMed: 2056131]

Baxter RC (2014) IGF binding proteins in cancer: mechanistic and clinical insights. Nat Rev Cancer, 14, 329–341. [PubMed: 24722429]

Bell JL, Wachter K, Muhleck B, Pazaitis N, Kohn M, Lederer M, & Huttelmaier S (2013) Insulin-like growth factor 2 mRNA-binding proteins (IGF2BPs): post-transcriptional drivers of cancer progression? Cell Mol Life Sci, 70, 2657–2675. [PubMed: 23069990]

Berenstein R, Blau O, Nogai A, Waechter M, Slonova E, Schmidt-Hieber M, Kunitz A, Pezzutto A, Doerken B, & Blau IW (2015) Multiple myeloma cells alter the senescence phenotype of bone marrow mesenchymal stromal cells under participation of the DLK1-DIO3 genomic region. BMC Cancer, 15, 68. [PubMed: 25886144]

Bieghs L, Brohus M, Kristensen IB, Abildgaard N, Bogsted M, Johnsen HE, Conover CA, De BE, Vanderkerken K, Overgaard MT, & Nyegaard M (2016a) Abnormal IGF-Binding Protein Profile in the Bone Marrow of Multiple Myeloma Patients. PLoS One, 11, e0154256. [PubMed: 27111220]

Bieghs L, Johnsen HE, Maes K, Menu E, Van VE, Overgaard MT, Nyegaard M, Conover CA, Vanderkerken K, & De BE (2016b) The insulin-like growth factor system in Multiple Myeloma: diagnostic and therapeutic potential. Oncotarget.

Boney CM, Moats-Staats BM, Stiles AD, & D'Ercole AJ (1994) Expression of insulin-like growth factor-I (IGF-I) and IGF-binding proteins during adipogenesis. Endocrinology, 135, 1863–1868. [PubMed: 7525256]

Boyd AL, Reid JC, Salci KR, Aslostovar L, Benoit YD, Shapovalova Z, Nakanishi M, Porras DP, Almakadi M, Campbell CJV, Jackson MF, Ross CA, Foley R, Leber B, Allan DS, Sabloff M, Xenocostas A, Collins TJ, & Bhatia M (2017) Acute myeloid leukaemia disrupts endogenous

myelo-erythropoiesis by compromising the adipocyte bone marrow niche. Nat Cell Biol, 19, 1336–1347. [PubMed: 29035359]

Bruns I, Cadeddu RP, Brueckmann I, Frobel J, Geyh S, Bust S, Fischer JC, Roels F, Wilk CM, Schildberg FA, Hunerliturkoglu AN, Zilkens C, Jager M, Steidl U, Zohren F, Fenk R, Kobbe G, Brors B, Czibere A, Schroeder T, Trumpp A, & Haas R (2012) Multiple myeloma-related deregulation of bone marrow-derived CD34(+) hematopoietic stem and progenitor cells. Blood, 120, 2620–2630. [PubMed: 22517906]

Cawthorn WP, Scheller EL, Learman BS, Parlee SD, Simon BR, Mori H, Ning X, Bree AJ, Schell B, Broome DT, Soliman SS, DelProposto JL, Lumeng CN, Mitra A, Pandit SV, Gallagher KA, Miller JD, Krishnan V, Hui SK, Bredella MA, Fazeli PK, Klibanski A, Horowitz MC, Rosen CJ, & MacDougald OA (2014) Bone marrow adipose tissue is an endocrine organ that contributes to increased circulating adiponectin during caloric restriction. Cell Metab, 20, 368–375. [PubMed: 24998914]

Corre J, Mahtouk K, Attal M, Gadelorge M, Huynh A, Fleury-Cappellesso S, Danho C, Laharrague P, Klein B, Reme T, & Bourin P (2007) Bone marrow mesenchymal stem cells are abnormal in multiple myeloma. Leukemia, 21, 1079–1088. [PubMed: 17344918]

Crane GM, Jeffery E, & Morrison SJ (2017) Adult haematopoietic stem cell niches. Nat Rev Immunol, 17, 573–590. [PubMed: 28604734]

Dabbah M, Attar-Schneider O, Zismanov V, Tartakover MS, Lishner M, & Drucker L (2016) Multiple myeloma cells promote migration of bone marrow mesenchymal stem cells by altering their translation initiation. J Leukoc. Biol 100, 761–770. [PubMed: 27272311]

DeMambro VE, Clemmons DR, Horton LG, Bouxsein ML, Wood TL, Beamer WG, Canalis E, & Rosen CJ (2008) Gender-specific changes in bone turnover and skeletal architecture in igfbp-2-null mice. Endocrinology, 149, 2051–2061. [PubMed: 18276763]

DeMambro VE, Le PT, Guntur AR, Maridas DE, Canalis E, Nagano K, Baron R, Clemmons DR, & Rosen CJ (2015) Igfbp2 Deletion in Ovariectomized Mice Enhances Energy Expenditure but Accelerates Bone Loss. Endocrinology, 156, 4129–4140. [PubMed: 26230658]

Doucette CR, Horowitz MC, Berry R, MacDougald OA, Anunciado-Koza R, Koza RA, & Rosen CJ (2015) A High Fat Diet Increases Bone Marrow Adipose Tissue (MAT) But Does Not Alter Trabecular or Cortical Bone Mass in C57BL/6J Mice. J Cell Physiol, 230, 2032–2037. [PubMed: 25663195]

Fairfield H, Falank C, Farrell M, Vary C, Boucher JM, Driscoll H, Liaw L, Rosen CJ, & Reagan MR (2018) Development of a 3D bone marrow adipose tissue model. Bone. 10.1016/j.bone.2018.01.023. [Epub ahead of print].

Fowler JA, Lwin ST, Drake MT, Edwards JR, Kyle RA, Mundy GR, & Edwards CM (2011) Host-derived adiponectin is tumor-suppressive and a novel therapeutic target for multiple myeloma and the associated bone disease. Blood, 118, 5872–5882. [PubMed: 21908434]

Frassanito MA, Rao L, Moschetta M, Ria R, Di ML, De LA, Racanelli V, Catacchio I, Berardi S, Basile A, Menu E, Ruggieri S, Nico B, Ribatti D, Fumarulo R, Dammacco F, Vanderkerken K, & Vacca A (2014) Bone marrow fibroblasts parallel multiple myeloma progression in patients and mice: in vitro and in vivo studies. Leukemia, 28, 904–916. [PubMed: 23995611]

Garcia-Gomez A, De Las RJ, Ocio EM, Diaz-Rodriguez E, Montero JC, Martin M, Blanco JF, Sanchez-Guijo FM, Pandiella A, San Miguel JF, & Garayoa M (2014) Transcriptomic profile induced in bone marrow mesenchymal stromal cells after interaction with multiple myeloma cells: implications in myeloma progression and myeloma bone disease. Oncotarget, 5, 8284–8305. [PubMed: 25268740]

Giuliani N, Ferretti M, Bolzoni M, Storti P, Lazzaretti M, Dalla PB, Bonomini S, Martella E, Agnelli L, Neri A, Ceccarelli F, & Palumbo C (2012) Increased osteocyte death in multiple myeloma patients: role in myeloma-induced osteoclast formation. Leukemia, 26, 1391–1401. [PubMed: 22289923]

Huynh H, Zheng J, Umikawa M, Zhang C, Silvany R, Iizuka S, Holzenberger M, Zhang W, & Zhang CC (2011) IGF binding protein 2 supports the survival and cycling of hematopoietic stem cells. Blood, 118, 3236–3243. [PubMed: 21821709]

Johnson SK, Stewart JP, Bam R, Qu P, Barlogie B, Van RF, Shaughnessy JD, Jr., Epstein J, & Yaccoby S (2014) CYR61/CCN1 overexpression in the myeloma microenvironment is associated with superior survival and reduced bone disease. Blood, 124, 2051–2060. [PubMed: 25061178]

Kobayashi H, Butler JM, O'Donnell R, Kobayashi M, Ding BS, Bonner B, Chiu VK, Nolan DJ, Shido K, Benjamin L, & Rafii S (2010) Angiocrine factors from Akt-activated endothelial cells balance self-renewal and differentiation of haematopoietic stem cells. Nat Cell Biol, 12, 1046–1056. [PubMed: 20972423]

Landgren O, Rajkumar SV, Pfeiffer RM, Kyle RA, Katzmann JA, Dispenzieri A, Cai Q, Goldin LR, Caporaso NE, Fraumeni JF, Blot WJ, & Signorello LB (2010) Obesity is associated with an increased risk of monoclonal gammopathy of undetermined significance among black and white women. Blood, 116, 1056–1059. [PubMed: 20421448]

Lawson MA, McDonald MM, Kovacic N, Hua KW, Terry RL, Down J, Kaplan W, Paton-Hough J, Fellows C, Pettitt JA, Neil DT, Van VE, Baldock PA, Rogers MJ, Eaton CL, Vanderkerken K, Pettit AR, Quinn JM, Zannettino AC, Phan TG, & Croucher PI (2015) Osteoclasts control reactivation of dormant myeloma cells by remodelling the endosteal niche. Nat Commun, 6, 8983. [PubMed: 26632274]

Li GW, Xu Z, Chen QW, Chang SX, Tian YN, & Fan JZ (2013) The temporal characterization of marrow lipids and adipocytes in a rabbit model of glucocorticoid-induced osteoporosis. Skeletal Radiol, 42, 1235–1244. [PubMed: 23754734]

Li X, Pennisi A, Zhan F, Sawyer JR, Shaughnessy JD, & Yaccoby S (2007) Establishment and exploitation of hyperdiploid and non-hyperdiploid human myeloma cell lines. Br J Haematol, 138, 802–811. [PubMed: 17760811]

Li X, Pennisi A, & Yaccoby S (2008) Role of decorin in the antimyeloma effects of osteoblasts. Blood, 112, 159–168. [PubMed: 18436739]

Li X, Ling W, Pennisi A, Wang Y, Khan S, Heidaran M, Pal A, Zhang X, He S, Zeitlin A, Abbot S, Faleck H, Hariri R, Shaughnessy JD, Jr., Van RF, Nair B, Barlogie B, Epstein J, & Yaccoby S (2011) Human placenta-derived adherent cells prevent bone loss, stimulate bone formation, and suppress growth of multiple myeloma in bone. Stem Cells, 29, 263–273. [PubMed: 21732484]

Li X, Ling W, Khan S, & Yaccoby S (2012) Therapeutic effects of intrabone and systemic mesenchymal stem cell cytotherapy on myeloma bone disease and tumor growth. J Bone Miner Res, 27, 1635–1648. [PubMed: 22460389]

Lv FJ, Tuan RS, Cheung KM, & Leung VY (2014) Concise review: the surface markers and identity of human mesenchymal stem cells. Stem Cells, 32, 1408–1419. [PubMed: 24578244]

Mattiucci D, Maurizi G, Izzi V, Cenci L, Ciarlantini M, Mancini S, Mensa E, Pascarella R, Vivarelli M, Olivieri A, Leoni P, & Poloni A (2018) Bone marrow adipocytes support hematopoietic stem cell survival. J Cell Physiol, 233, 1500–1511. [PubMed: 28574591]

Morris EV & Edwards CM (2018) Bone marrow adiposity and multiple myeloma. Bone, 10.1016/j.bone.2018.03.011. [Epub ahead of print].

Morrison SJ & Scadden DT (2014) The bone marrow niche for haematopoietic stem cells. Nature, 505, 327–334. [PubMed: 24429631]

Nair B, Van RF, Shaughnessy JD, Jr., Anaissie E, Szymonifka J, Hoering A, Alsayed Y, Waheed S, Crowley J, & Barlogie B (2010) Superior results of Total Therapy 3 (2003–33) in gene expression profiling-defined low-risk multiple myeloma confirmed in subsequent trial 2006–66 with VRD maintenance. Blood, 115, 4168–4173. [PubMed: 20124509]

Nair S, Branagan AR, Liu J, Boddupalli CS, Mistry PK, & Dhodapkar MV (2016) Clonal Immunoglobulin against Lysolipids in the Origin of Myeloma. N Engl J Med, 374, 555–561. [PubMed: 26863356]

Naveiras O, Nardi V, Wenzel PL, Hauschka PV, Fahey F, & Daley GQ (2009) Bone-marrow adipocytes as negative regulators of the haematopoietic microenvironment. Nature, 460, 259–263. [PubMed: 19516257]

Noll JE, Williams SA, Tong CM, Wang H, Quach JM, Purton LE, Pilkington K, To LB, Evdokiou A, Gronthos S, & Zannettino AC (2014) Myeloma plasma cells alter the bone marrow microenvironment by stimulating the proliferation of mesenchymal stromal cells. Haematologica, 99, 163–171. [PubMed: 23935020]

Paiva B, Perez-Andres M, Vidriales MB, Almeida J, de Las HN, Mateos MV, Lopez-Corral L, Gutierrez NC, Blanco J, Oriol A, Hernandez MT, de AF, de Coca AG, Terol MJ, de la Rubia J, Gonzalez Y, Martin A, Sureda A, Schmidt-Hieber M, Schmitz A, Johnsen HE, Lahuerta JJ, Blade J, San-Miguel JF, & Orfao A (2011) Competition between clonal plasma cells and normal cells for potentially overlapping bone marrow niches is associated with a progressively altered cellular distribution in MGUS vs myeloma. Leukemia, 25, 697–706. [PubMed: 21252988]

Pennisi A, Ling W, Li X, Khan S, Shaughnessy JD, Jr., Barlogie B, & Yaccoby S (2009) The ephrinB2/EphB4 axis is dysregulated in osteoprogenitors from myeloma patients and its activation affects myeloma bone disease and tumor growth. Blood, 114, 1803–1812. [PubMed: 19597185]

Pickard A & McCance DJ (2015) IGF-Binding Protein 2 - Oncogene or Tumor Suppressor? Front Endocrinol (Lausanne.), 6, 25. [PubMed: 25774149]

Rahman S, Lu Y, Czernik PJ, Rosen CJ, Enerback S, & Lecka-Czernik B (2013) Inducible brown adipose tissue, or beige fat, is anabolic for the skeleton. Endocrinology, 154, 2687–2701. [PubMed: 23696565]

Reagan MR, Mishima Y, Glavey SV, Zhang Y, Manier S, Lu ZN, Memarzadeh M, Zhang Y, Sacco A, Aljawai Y, Shi J, Tai YT, Ready JE, Kaplan DL, Roccaro AM, & Ghobrial IM (2014) Investigating osteogenic differentiation in multiple myeloma using a novel 3D bone marrow niche model. Blood. 124, 3250–3259. [PubMed: 25205118]

Scheller EL, Doucette CR, Learman BS, Cawthorn WP, Khandaker S, Schell B, Wu B, Ding SY, Bredella MA, Fazeli PK, Khoury B, Jepsen KJ, Pilch PF, Klibanski A, Rosen CJ, & MacDougald OA (2015) Region-specific variation in the properties of skeletal adipocytes reveals regulated and constitutive marrow adipose tissues. Nat Commun, 6, 7808. [PubMed: 26245716]

Scheller EL, Khoury B, Moller KL, Wee NK, Khandaker S, Kozloff KM, Abrishami SH, Zamarron BF, & Singer K (2016) Changes in Skeletal Integrity and Marrow Adiposity during High-Fat Diet and after Weight Loss. Front Endocrinol (Lausanne.), 7, 102. [PubMed: 27512386]

Schinke C, Qu P, Mehdi SJ, Hoering A, Epstein J, Johnson S, Van RF, Zangari M, Thanendrarajan S, Barlogie B, Davies FE, Yaccoby S, & Morgan G (2018) The pattern of Mesenchymal stem cell expression is an independent marker of outcome in multiple myeloma. Clin Cancer Res, 24, 2913–2919. [PubMed: 29563136]

Shafat MS, Oellerich T, Mohr S, Robinson SD, Edwards DR, Marlein CR, Piddock RE, Fenech M, Zaitseva L, Abdul-Aziz A, Turner J, Watkins JA, Lawes M, Bowles KM, & Rushworth SA (2017) Leukemic blasts program bone marrow adipocytes to generate a protumoral microenvironment. Blood, 129, 1320–1332. [PubMed: 28049638]

Shaughnessy JD, Jr., Zhan F, Burington BE, Huang Y, Colla S, Hanamura I, Stewart JP, Kordsmeier B, Randolph C, Williams DR, Xiao Y, Xu H, Epstein J, Anaissie E, Krishna SG, Cottler-Fox M, Hollmig K, Mohiuddin A, Pineda-Roman M, Tricot G, Van RF, Sawyer J, Alsayed Y, Walker R, Zangari M, Crowley J, & Barlogie B (2007) A validated gene expression model of high-risk multiple myeloma is defined by deregulated expression of genes mapping to chromosome 1. Blood, 109, 2276–2284. [PubMed: 17105813]

Slany A, Haudek-Prinz V, Meshcheryakova A, Bileck A, Lamm W, Zielinski C, Gerner C, & Drach J (2014) Extracellular matrix remodeling by bone marrow fibroblast-like cells correlates with disease progression in multiple myeloma. J Proteome. Res, 13, 844–854. [PubMed: 24256566]

Trotter TN, Gibson JT, Sherpa TL, Gowda PS, Peker D, & Yang Y (2016) Adipocyte-Lineage Cells Support Growth and Dissemination of Multiple Myeloma in Bone. Am J Pathol, 186, 3054–3063. [PubMed: 27648615]

Vacca A, Ria R, Reale A, & Ribatti D (2014) Angiogenesis in multiple myeloma. Chem. Immunol Allergy, 99, 180–196. [PubMed: 24217610]

van Rhee F, Mitchell A, Heuck C, Grazziutti M, Jethava Y, Khan RZ, & Johann D (2014) Total Therapy 4 (TT4) for GEP70-Defined Low Risk Clinical Multiple Myeloma (CMM): Results of Patients Randomized to a Standard v Light Rrm (S-TT4 v L-TT4). 124, 3403 2014 Blood, 124, 1199.

Xi G, Wai C, DeMambro V, Rosen CJ, & Clemmons DR (2014) IGFBP-2 directly stimulates osteoblast differentiation. J Bone Miner Res, 29, 2427–2438. [PubMed: 24839202]

Xu S, De VK, De BA, Vanderkerken K, & Van RI (2018) Mesenchymal stem cells in multiple myeloma: a therapeutical tool or target? Leukemia, 32, 1500–1514. [PubMed: 29535427]

Yaccoby S (2010a) Advances in the understanding of myeloma bone disease and tumour growth. Br J Haematol, 149, 311–321. [PubMed: 20230410]

Yaccoby S (2010b) Osteoblastogenesis and tumor growth in myeloma. Leuk. Lymphoma, 51, 213–220. [PubMed: 20038269]

Yaccoby S, Wezeman MJ, Zangari M, Walker R, Cottler-Fox M, Gaddy D, Ling W, Saha R, Barlogie B, Tricot G, & Epstein J (2006) Inhibitory effects of osteoblasts and increased bone formation on myeloma in novel culture systems and a myelomatous mouse model. Haematologica, 91, 192–199. [PubMed: 16461303]

Zhan F, Huang Y, Colla S, Stewart JP, Hanamura I, Gupta S, Epstein J, Yaccoby S, Sawyer J, Burington B, Anaissie E, Hollmig K, Pineda-Roman M, Tricot G, Van RF, Walker R, Zangari M, Crowley J, Barlogie B, & Shaughnessy JD, Jr. (2006) The molecular classification of multiple myeloma. Blood, 108, 2020–2028. [PubMed: 16728703]

Zhou BO, Yu H, Yue R, Zhao Z, Rios JJ, Naveiras O, & Morrison SJ (2017) Bone marrow adipocytes promote the regeneration of stem cells and haematopoiesis by secreting SCF. Nat Cell Biol, 19, 891–903. [PubMed: 28714970]

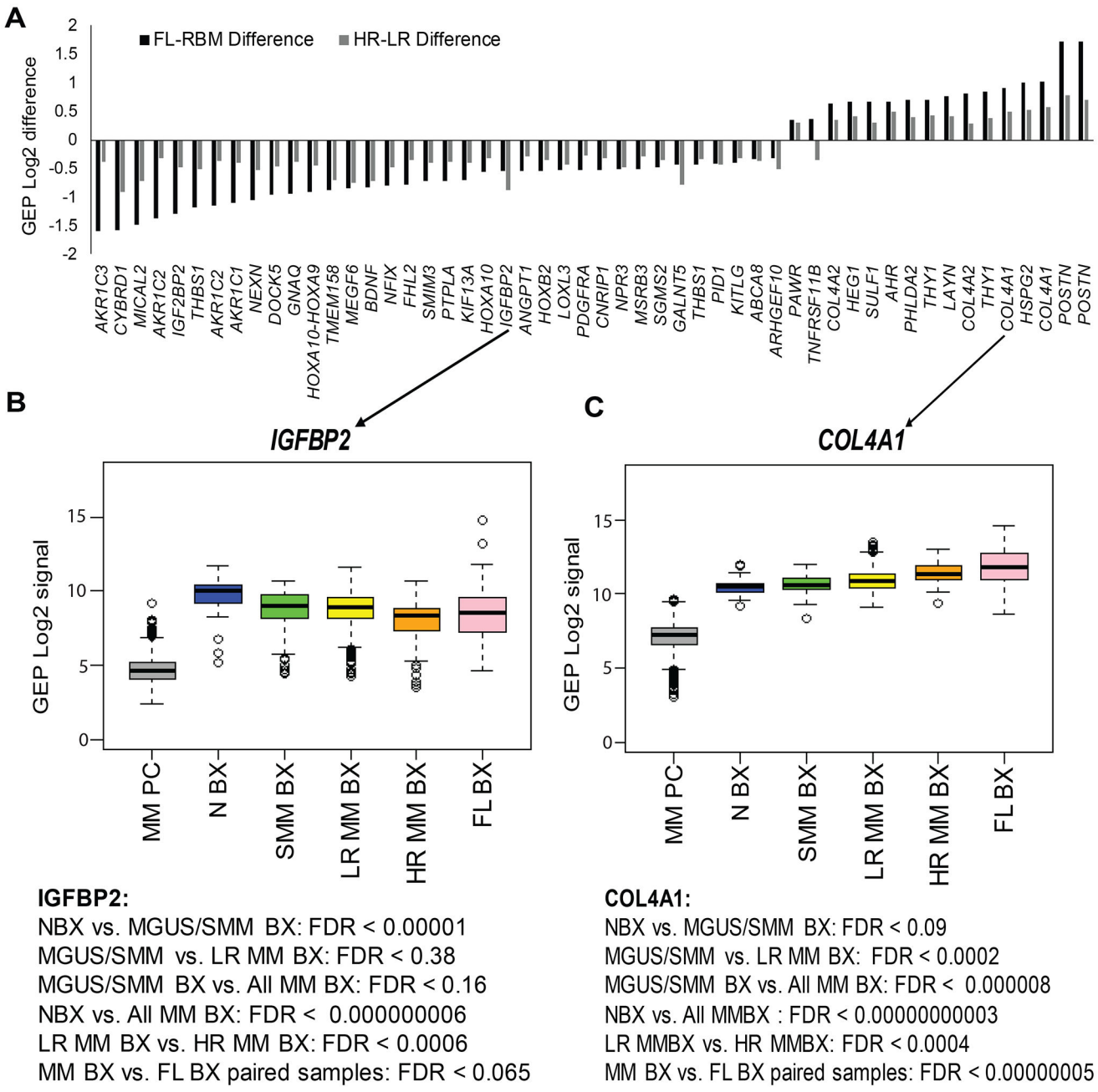

IGFBP2:
NBX vs. MGUS/SMM BX: FDR < 0.00001
MGUS/SMM vs. LR MM BX: FDR < 0.38
MGUS/SMM BX vs. All MM BX: FDR < 0.16
NBX vs. All MM BX: FDR < 0.000000006
LR MM BX vs. HR MM BX: FDR < 0.0006
MM BX vs. FL BX paired samples: FDR < 0.065

COL4A1:
NBX vs. MGUS/SMM BX: FDR < 0.09
MGUS/SMM vs. LR MM BX: FDR < 0.0002
MGUS/SMM BX vs. All MM BX: FDR < 0.000008
NBX vs. All MMBX : FDR < 0.00000000003
LR MMBX vs. HR MMBX: FDR < 0.0004
MM BX vs. FL BX paired samples: FDR < 0.00000005

Fig 1. Expression of MSC genes linked to adipocytes and angiogenesis was altered in whole-bone biopsies of MM patients with high-risk disease and in FLs.

(**A**) Expression levels of probe sets differentially expressed in mesenchymal stem cells (MSCs) of paired biopsy samples (i.e., two samples from the same patient) from focal lesions (FLs) versus random bone marrow (RBM), and in patients with high-risk versus low-risk multiple myeloma (MM). The probe sets are listed based on a false discovery rate (FDR) < 0.1 and expression difference > or < log2 0.25 between the tested groups. Note, in samples from patients with MM, of several genes associated with adipocytes (e.g. *IGFBP2, AKR1C3*) were downregulated and genes associated with angiogenesis (e.g. *COL4A1,*

HSPG2) were upregulated. (**B**) Mean expression of *IGFBP2* and *COL4A1* is shown for MM plasma cells (MM PC; negative control) and for biopsies from healthy donors (N BX, n = 68); from patients with smouldering MM (SMM BX, n = 52), low-risk MM (LR MM BX, n = 467), and high-risk MM (HR MM BX, n = 64); and from FLs (FL BX, n = 178). Note gradual changes in expression of these genes at different disease stages of MM. GEP: gene expression profiling;

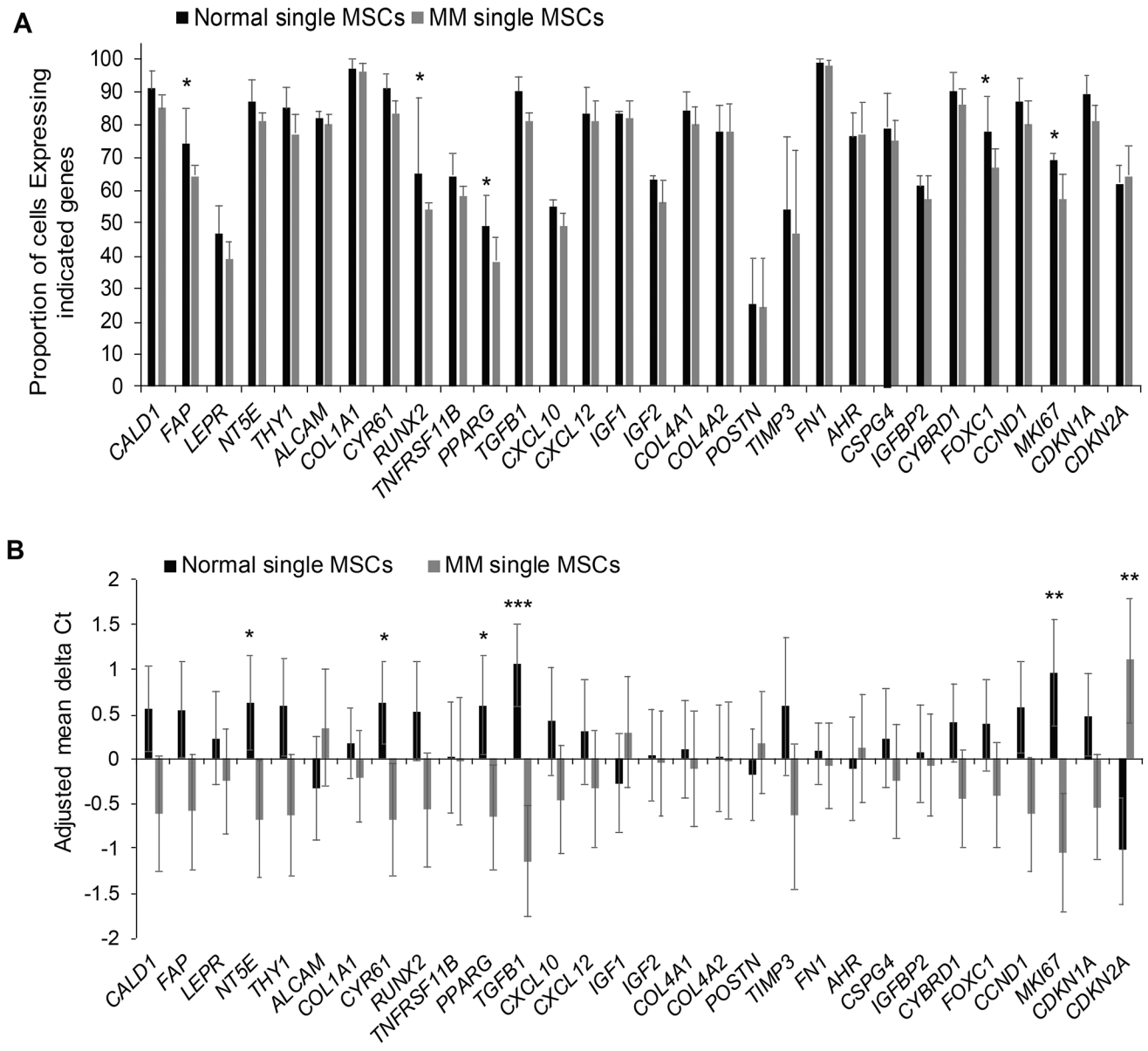

Fig 2. Individual bone marrow MSCs express MSC genes at heterogeneous levels that are influenced by MM.

Expression (mean ± SEM) of indicated genes analysed in single mesenchymal stem cells (MSCs)from three healthy donors (n = 175) and three patients with multiple myeloma (MM; n = 162). (**A**) Proportion (%) of single MSCs expressing indicated genes. *Genes in which the differential proportion between the two groups is > 10%. (**B**) Adjusted mean delta Ct (ΔCt) for single MSCs from patients with MM versus those from healthy donors were calculated by subtracting ΔCt of each gene with the mean of ΔCt of total cells. Gene expression was highly variable in individual MSCs, and expression of only a few genes (e.g., *MKI67, CDKN2A*) was significantly different between the two groups. * p<0.05; ** p<0.01; *** p<0.002.

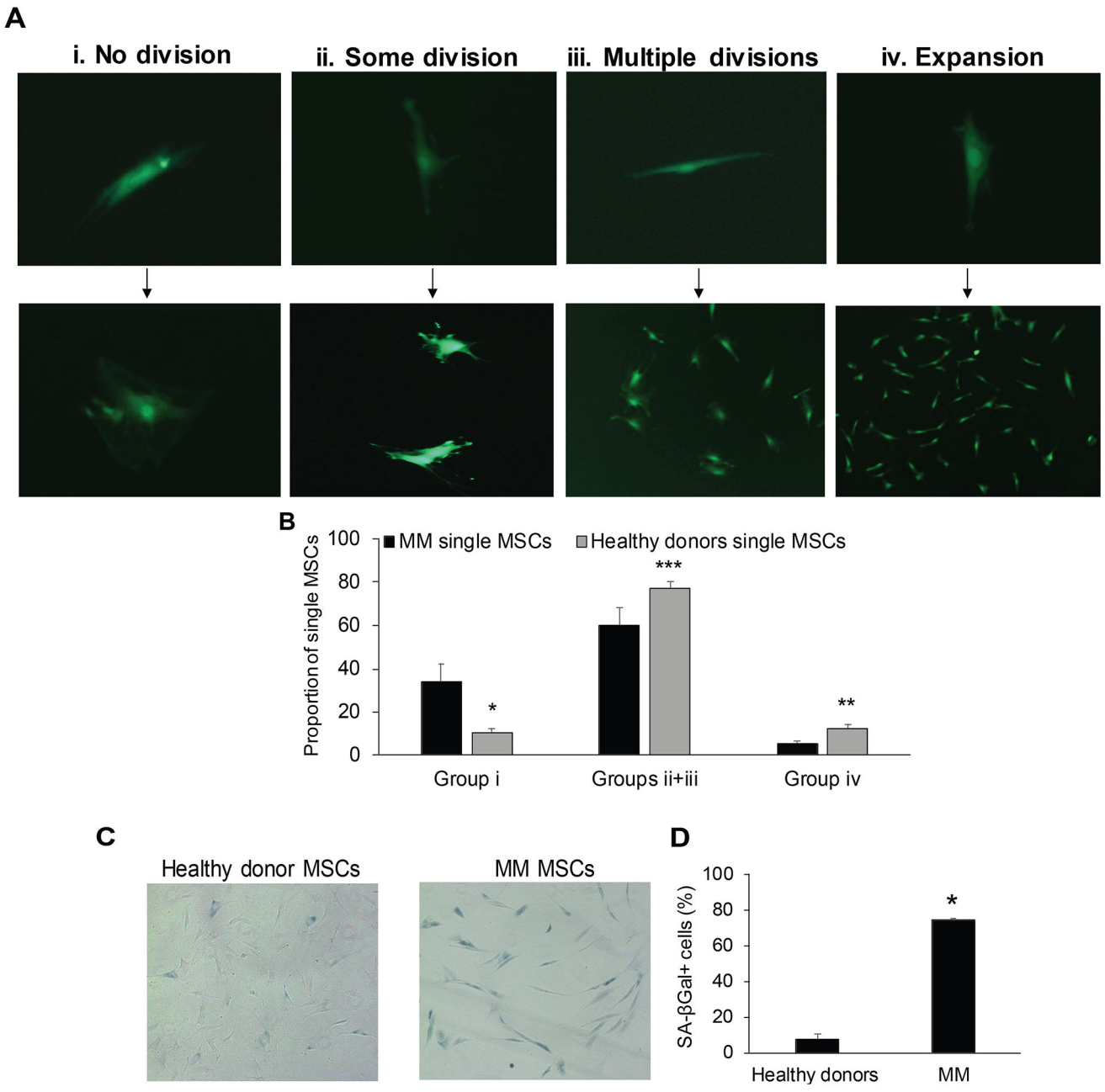

Fig 3. Individual MSCs from BM of MM patients have reduced proliferative potential and higher expression of senescence-associated (SA) marker βGal.

Individual mesenchymal stem cells (MSCs)from age-matched healthy donors (n = 3) and patients with multiple myeloma (MM; n = 3) were cultured for at least 4 weeks. (**A**) Growth pattern of single MSCs was segregated into 4 groups: MSCs that did not divide (i), MSCs that divided only once (ii), MSCs that divided a few times and stopped (iii) and MSCs that were capable of expanding and generating MSC lines (iv). (**B**) Proportion of single MSCs in groups i, ii + iii and iv. * p<0.03; ** p<0.01; *** p<0.07. (**C**, **D**) Unexpanded MSCs from age-matched healthy donors (n = 3) and patients with MM (n = 3) were stained with SA-βGal. *** p<0.0001**. Images were obtained with a Zeiss AX10 Observer.A1 microscope (Carl

Zeiss Microimaging Gmbh, Göttingen, Germany) equipped with infinity 3 camera (Lumenera, Ontario, Canada).

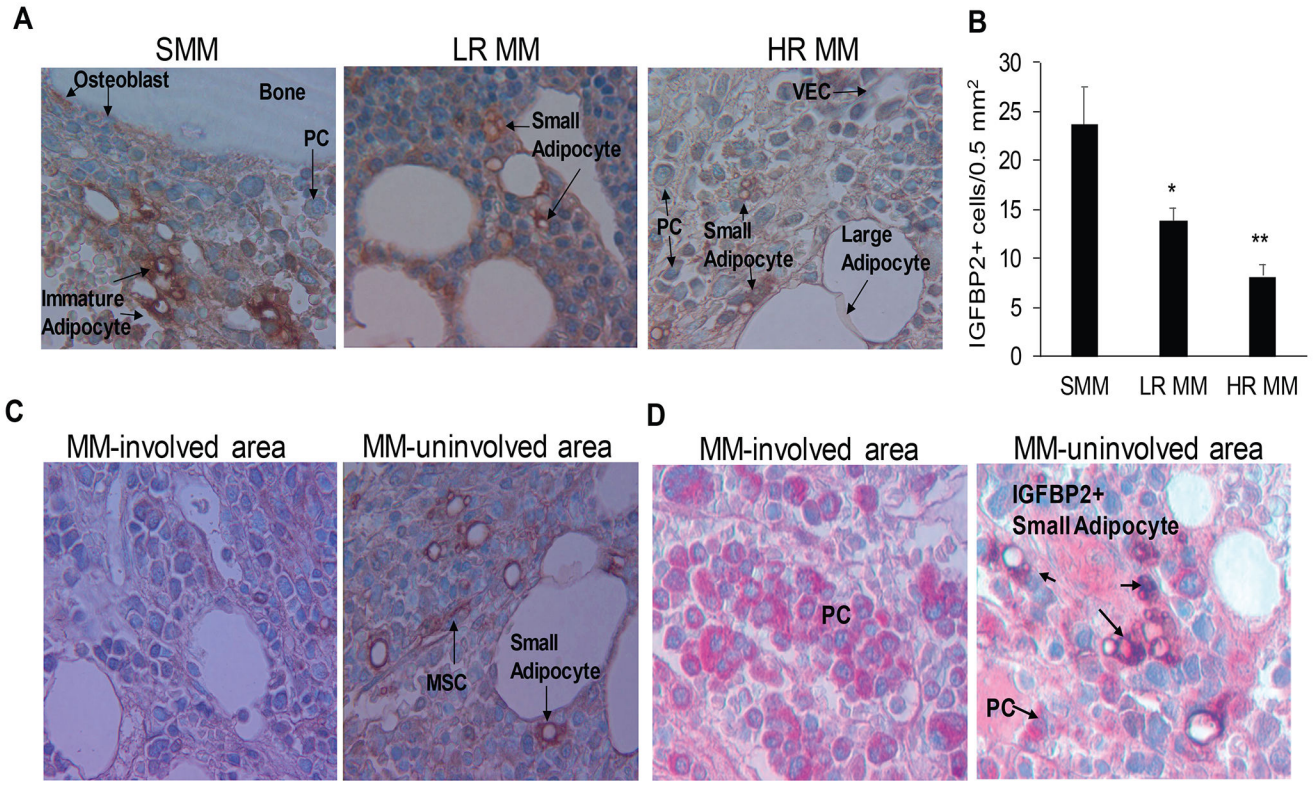

Fig 4. Mesenchymal cells that express IGFBP2 and exhibit morphology of small adipocytes are lower in BM from patients with MM than in that from patients with SMM.

(**A**, **B**) Biopsy bone sections from patients with smouldering multiple myeloma (SMM; n=10), low-risk (LR) MM (n=10), and high-risk (HR) MM (n=10) were immunohistochemically stained for IGFBP2 (brown); positive cells were quantified. (**C**) Biopsy sample from a patient with MM that illustrates differences in frequency of IGFBP2+ cells in a MM-involved area (left panel) and a MM-uninvolved area (right panel). (**D**) Biopsy sample from a MM patient that was doubled-stained for IGFBP2 (brown) and Ig lambda (red). Note IGFBP2+ cells in MM-uninvolved area (right panel) compared to MM-involved area (left panel). (MSC: mesenchymal stem cell; PC: plasma cell; VEC: vascular endothelial cell). * $p<0.02$ vs. SMM; ** $p<0.015$ vs. LR. Images were obtained with an Olympus BH2 microscope equipped with a 160 x/0.17 numerical aperture objective (Olympus, Melville, NY); original magnification, 200×. Images were acquired with a SPOT2 digital camera (Diagnostic Instruments, Sterling Heights, MI, USA) and were processed with Adobe Photoshop version 11 (Adobe Systems, San Jose, CA, USA).

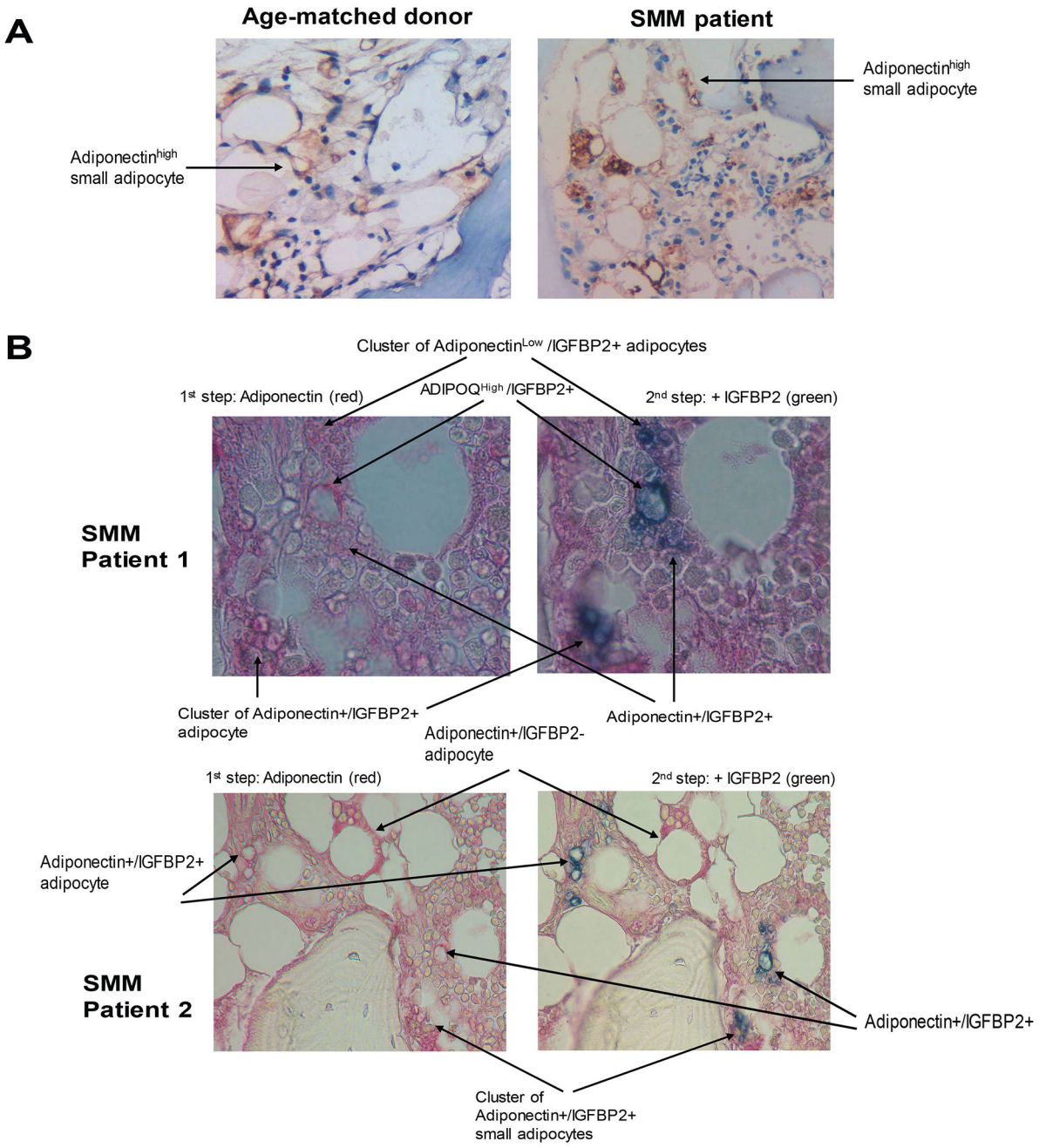

Fig 5. A subset of BM adipocytes co-express IGFBP2 and adiponectin.

(**A**) Immunohistochemical staining of adiponectin (stained brown) in bone sections from a healthy donor and a patient with smouldering multiple myeloma (SMM). (**B**) Sequential immunohistochemical staining for adiponectin (stained red) and IGFBP2 (stained green) in bone sections from patients with SMM. Note that cells positive for both markers are dark blue (red + green merging colour). Images were obtained with an Olympus BH2 microscope equipped with a 160 x/0.17 numerical aperture objective; original magnification, 200×. Images were acquired with a SPOT2 digital camera and were processed with Adobe Photoshop version 11.

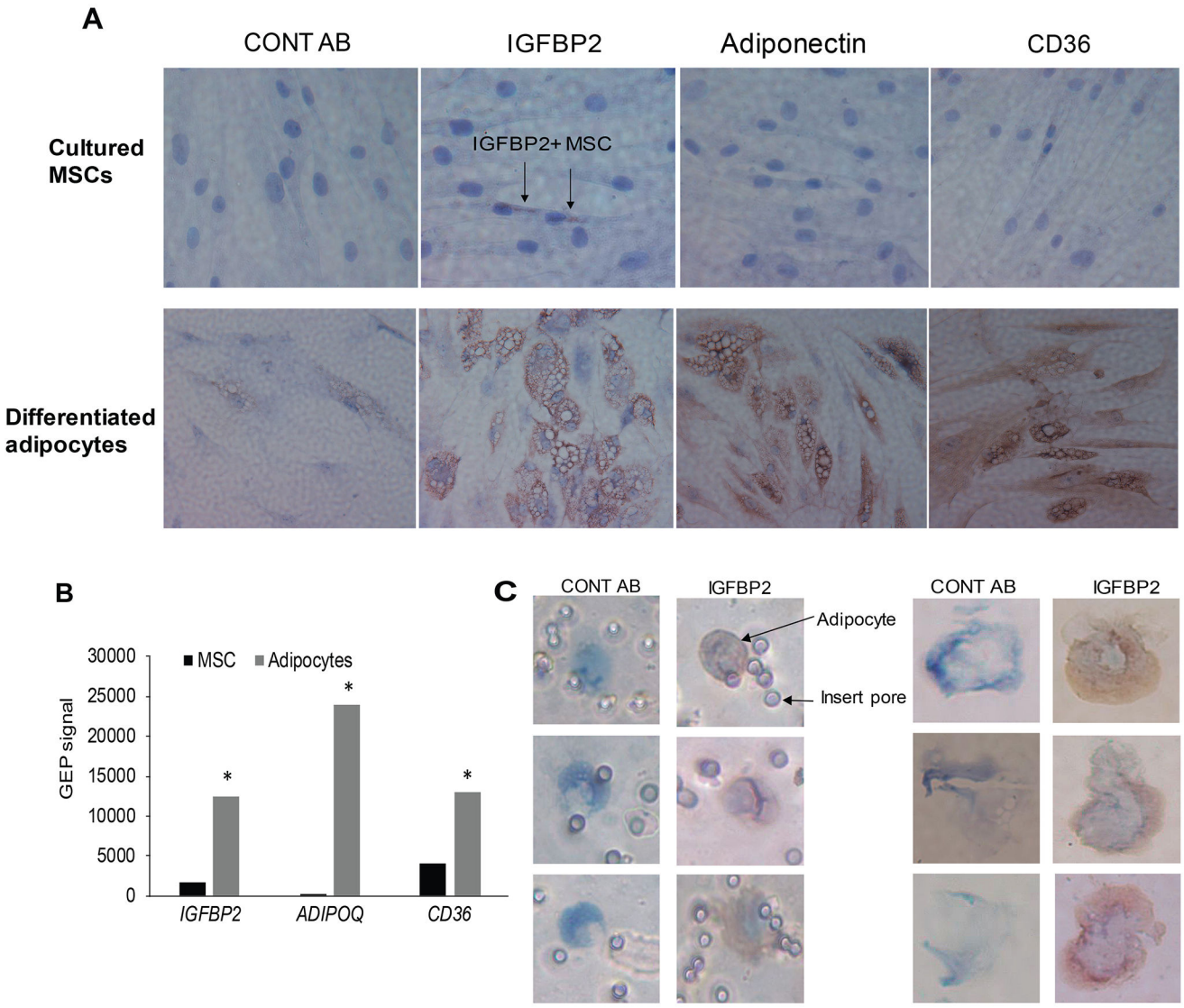

Fig 6. Primary and cultured adipocytes express IGFBP2.

(**A**) Normal MSCs and their differentiated adipocytes were immunohistochemically stained (brown) for nonspecific antibody (CONT AB), IGFBP2, adiponectin and CD36. (**B**) Expression (determined by GEP) of genes encoding IGFBP2, adiponectin, and CD36 in MSCs and their differentiated adipocytes. *** p<0.03**. (**C**) Individual primary adipocytes were captured on culture Transwell inserts (left panel) or with cytospin (right panel) and then immunohistochemically stained for IGFBP2. Images were obtained with an Olympus BH2 microscope equipped with a 160 x/0.17 numerical aperture objective; original magnification, 400×. Images were acquired with a SPOT2 digital camera and were processed with Adobe Photoshop version 11.

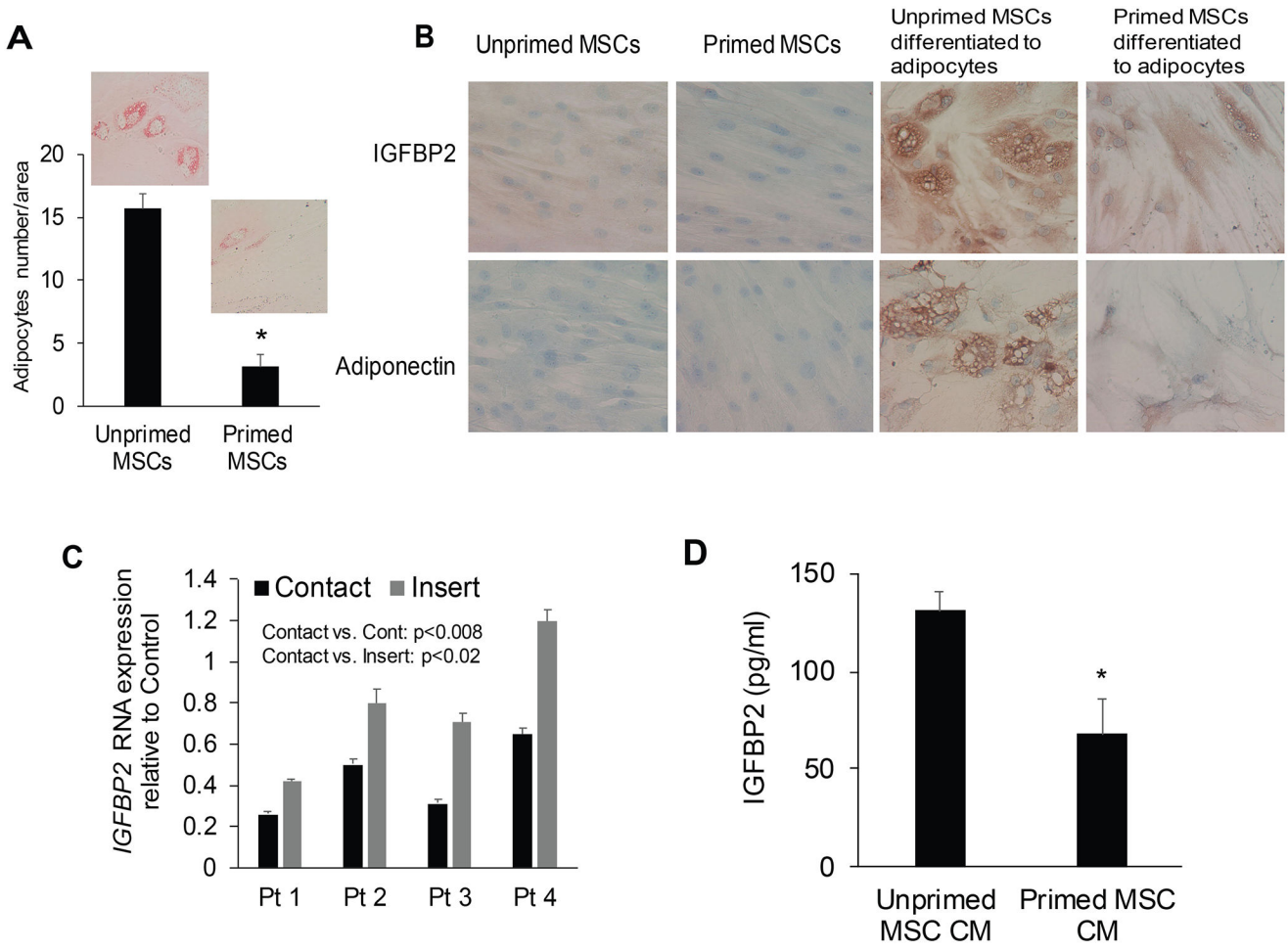

Fig 7. Priming MSCs with MM cells suppresses their differentiation potential to adipocytes and reduces their expression of IGFBP2.

(**A**) Large adipocytes (stained with Oil Red O) were enumerated in unprimed (cultured in absence of multiple myeloma) and primed mesenchymal stem cells (MSCs)after their differentiation into adipocytes. *** p<0.001**. (**B**) Immunohistochemical staining (brown) for IGFBP2 and adiponectin in unprimed and primed MSCs and their differentiated adipocytes. (**c**) Normal MSCs were co-cultured with MM cells from 4 patients in conditions with or without cell-cell contact (culture inserts inhibited contact) or cultured alone (control) for 3 days. Expression of *IGFBP2* was analysed with real time quantitative reverse transcription polymerase chain reaction. (**d**) Level of IGFBP2 in conditioned media (CM) of unprimed and primed MSCs. *** p<0.004**.

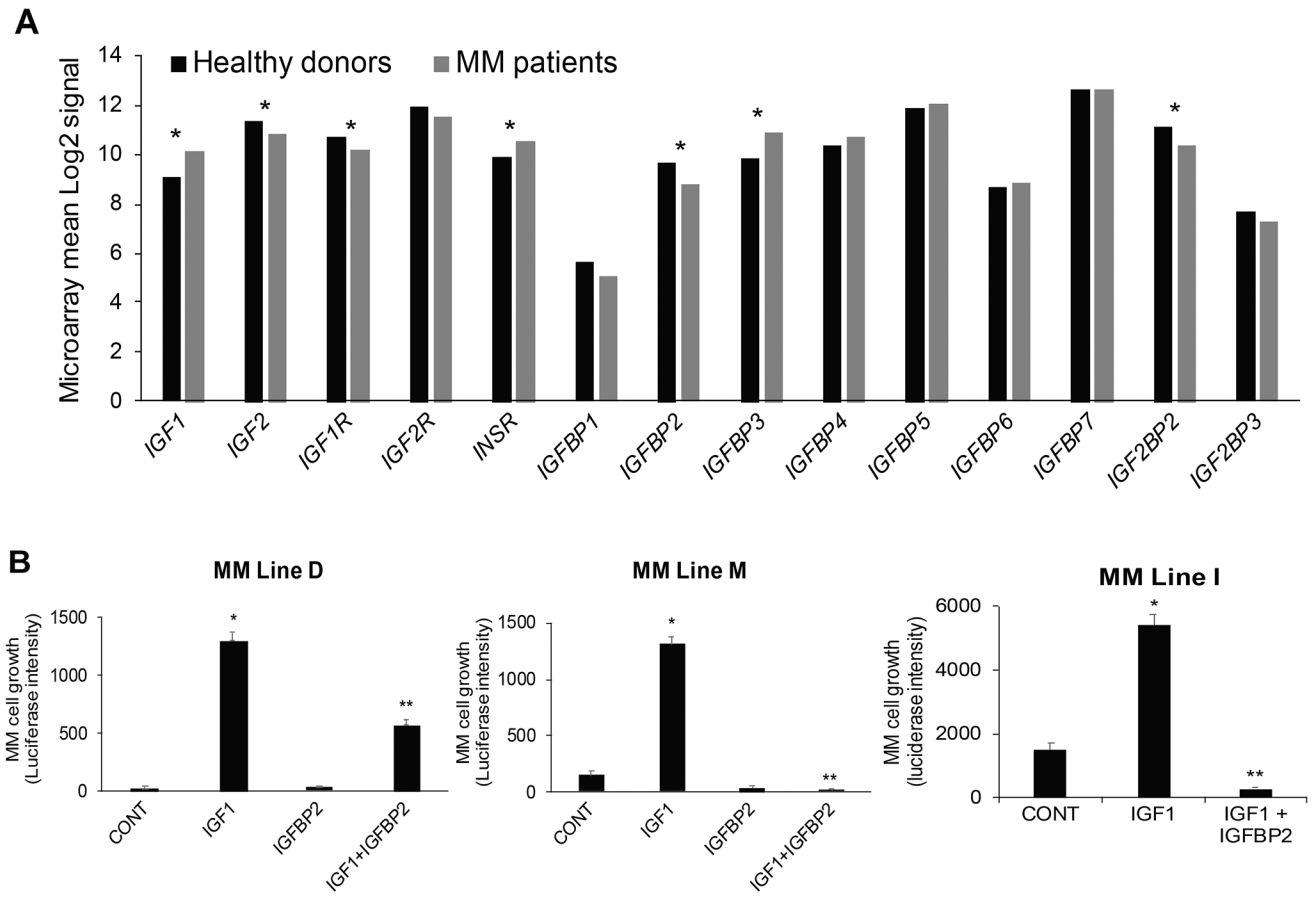

Fig 8. IGFBP2 is negatively impacted by MM and is a suppressor of IGF1-induced MM cell growth.

(**a**) Expression of genes related to the IGF axis (ligands, receptors, binding proteins) in biopsy samples of healthy donors and multiple myeloma (MM) patients; * $p < 0.05$. (**b**) Growth of three luciferase-expressing bone marrow-dependent MM cell lines, M, D and I, cultured in serum-free conditions for 48 h in the absence and presence of IGF1 (40 ng/ml) and IGFBP2 (5 μg/ml). * $p<0.0001$ vs. control (CONT); ** $p<0003$ vs. IGF1.